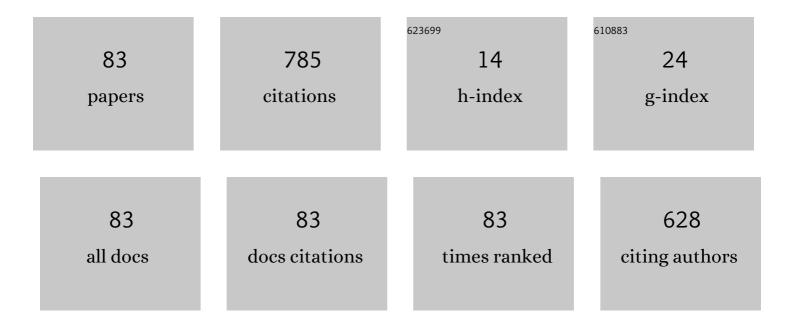
Yongzhao Yao Yao

List of Publications by Year in descending order

Source: https://exaly.com/author-pdf/6102485/publications.pdf Version: 2024-02-01



#	Article	IF	CITATIONS
1	A synchrotron X-ray topography study of crystallographic defects in ScAlMgO4 single crystals. Journal of Alloys and Compounds, 2022, 896, 163025.	5.5	5
2	Three-dimensional curving of crystal planes in wide bandgap semiconductor wafers visualized using a laboratory X-ray diffractometer. Journal of Crystal Growth, 2022, 583, 126558.	1.5	2
3	Mechanism of molten KOH+NaOH etching of GaN revealed by the slopes of etch pits formed at threading dislocations. Journal of Alloys and Compounds, 2022, 902, 163830.	5.5	5
4	Etch pit formation on β-Ga2O3 by molten KOH+NaOH and hot H3PO4 and their correlation with dislocations. Journal of Alloys and Compounds, 2022, 910, 164788.	5.5	5
5	Observation of dislocations in thick î² -Ga2O3 single-crystal substrates using Borrmann effect synchrotron x-ray topography. APL Materials, 2022, 10, .	5.1	8
6	Observation of threading dislocations with a c+m type Burgers vector in HVPE GaN substrates using multi-photon excitation photoluminescence and TEM. Journal of Crystal Growth, 2022, , 126748.	1.5	0
7	Size of dislocation patterns induced by Vickers indentation in hydride vapor-phase epitaxy GaN. Journal of Applied Physics, 2022, 131, .	2.5	7
8	Large-area total-thickness imaging and Burgers vector analysis of dislocations in <i>β</i> -Ga2O3 using bright-field x-ray topography based on anomalous transmission. Applied Physics Letters, 2022, 121, .	3.3	5
9	Preparation of crystalline SiC coating from Si and C powder mixture using laser sublimation technique. Journal of the Ceramic Society of Japan, 2021, 129, 310-314.	1.1	0
10	Generation of dislocations from scratches on GaN formed during wafer fabrication and dislocation reactions during homoepitaxial growth. Japanese Journal of Applied Physics, 2021, 60, 115501.	1.5	5
11	X-ray topography of crystallographic defects in wide-bandgap semiconductors using a high-resolution digital camera. Japanese Journal of Applied Physics, 2021, 60, 010908.	1.5	4
12	Deep ultraviolet emission from multiple quantum wells on flat N-polar AlN templates fabricated using periodical pulsed H ₂ etching. Japanese Journal of Applied Physics, 2021, 60, 125502.	1.5	4
13	Visualization of the curving of crystal planes in β-Ga2O3 by X-ray topography. Journal of Crystal Growth, 2021, 576, 126376.	1.5	4
14	Anisotropic radius of curvature of crystal planes in wide-bandgap semiconductor wafers measured by X-ray diffraction. Japanese Journal of Applied Physics, 2021, 60, 128004.	1.5	2
15	Revelation of Dislocations in βâ€Ga ₂ O ₃ Substrates Grown by Edgeâ€Đefined Filmâ€Fed Growth. Physica Status Solidi (A) Applications and Materials Science, 2020, 217, 1900630.	1.8	23
16	Three-Dimensional Observation of Internal Defects in a β-Ga2O3 (001) Wafer Using the FIB–SEM Serial Sectioning Method. Journal of Electronic Materials, 2020, 49, 5190-5195.	2.2	9
17	Dislocation classification of a large-area β-Ga2O3 single crystal via contrast analysis of affine-transformed X-ray topographs. Journal of Crystal Growth, 2020, 548, 125825.	1.5	6
18	Correlation between structural properties and nonradiative recombination behaviors of threading dislocations in freestanding GaN substrates grown by hydride vapor phase epitaxy. CrystEngComm, 2020, 22, 8299-8312.	2.6	13

Υονςζήλο Υλό Υλο

#	Article	IF	CITATIONS
19	Study of dislocations in AlN single-crystal using bright-field synchrotron x-ray topography under a multiple-beam diffraction condition. Applied Physics Letters, 2020, 117, 092102.	3.3	4
20	Decreased Mortality with Beta-Blocker Therapy in HFpEF Patients Associated with Atrial Fibrillation. Cardiology Research and Practice, 2020, 2020, 1-7.	1.1	6
21	Identification of Burgers vectors of dislocations in monoclinic \hat{I}^2 -Ga2O3 via synchrotron x-ray topography. Journal of Applied Physics, 2020, 127, .	2.5	24
22	Observation of dislocations in β-Ga2O3 single-crystal substrates by synchrotron X-ray topography, chemical etching, and transmission electron microscopy. Japanese Journal of Applied Physics, 2020, 59, 045502.	1.5	18
23	Mg diffusion and activation along threading dislocations in GaN. Applied Physics Letters, 2020, 116, .	3.3	12
24	Revelation of Dislocations in βâ€Ga ₂ O ₃ Substrates Grown by Edgeâ€Defined Filmâ€Fed Growth. Physica Status Solidi (A) Applications and Materials Science, 2020, 217, 2070016.	1.8	2
25	Growth and Characterization of Nitrogenâ€Polar AlGaN/AlN Heterostructure for Highâ€Electronâ€Mobility Transistor. Physica Status Solidi (B): Basic Research, 2020, 257, 1900589.	1.5	13
26	Growth of Nâ€Polar Aluminum Nitride on Vicinal Sapphire Substrates and Aluminum Nitride Bulk Substrates. Physica Status Solidi (B): Basic Research, 2020, 257, 1900588.	1.5	17
27	Crystallinity Evaluation and Dislocation Observation for an Aluminum Nitride Single-Crystal Substrate on a Wafer Scale. Journal of Electronic Materials, 2020, 49, 5144-5153.	2.2	7
28	Screw dislocations on \$left{1ar{2}12ight}\$ pyramidal planes induced by Vickers indentation in HVPE GaN. Japanese Journal of Applied Physics, 2020, 59, 091005.	1.5	11
29	Slip planes in monoclinic β-Ga ₂ O ₃ revealed from its {010} face via synchrotron X-ray diffraction and X-ray topography. Japanese Journal of Applied Physics, 2020, 59, 125501.	1.5	18
30	Identification of fine structures at the surface of epi-ready GaN wafer observed by confocal differential interference contrast microscopy. Japanese Journal of Applied Physics, 2020, 59, 100907.	1.5	1
31	Observation of dislocations and their arrays in physical vapor transport-grown AlN single-crystal substrate by synchrotron X-ray topography. Japanese Journal of Applied Physics, 2019, 58, SCCB29.	1.5	10
32	X-ray diffraction and Raman characterization of Î ² -Ga2O3 single crystal grown by edge-defined film-fed growth method. Journal of Applied Physics, 2019, 126, .	2.5	29
33	Observation of Threading Dislocations in Ammonothermal Gallium Nitride Single Crystal Using Synchrotron X-ray Topography. Journal of Electronic Materials, 2018, 47, 5007-5012.	2.2	28
34	Correlation between dislocations and leakage current of p-n diodes on a free-standing GaN substrate. Applied Physics Letters, 2018, 112, .	3.3	142
35	Expansion of Basal Plane Dislocation in 4H-SiC Epitaxial Layer on A-Plane by Electron Beam Irradiation. Materials Science Forum, 2018, 924, 151-154.	0.3	1
36	Expansion of a single Shockley stacking fault in a 4H-SiC (112Â ⁻ 0) epitaxial layer caused by electron beam irradiation. Journal of Applied Physics, 2018, 123, .	2.5	27

Υονςζήλο Υλό Υλό

#	Article	IF	CITATIONS
37	Characterization of threading dislocations in GaN (0001) substrates by photoluminescence imaging, cathodoluminescence mapping and etch pits. Journal of Crystal Growth, 2017, 468, 484-488.	1.5	22
38	Dislocations in SiC Revealed by NaOH Vapor Etching and a Comparison with X-Ray Topography Taken with Various <i>g</i> -Vectors. Materials Science Forum, 2016, 858, 389-392.	0.3	1
39	Revelation of dislocations in HVPE GaN single crystal by KOH etching with Na2O2 additive and cathodoluminescence mapping. Superlattices and Microstructures, 2016, 99, 83-87.	3.1	33
40	Fast removal of surface damage layer from single crystal diamond by using chemical etching in molten KCl + KOH solution. Diamond and Related Materials, 2016, 63, 86-90.	3.9	7
41	Therapeutic delivery of cyclin-A2 via recombinant adeno-associated virus serotype 9 restarts the myocardial cell cycle: An in vitro study. Molecular Medicine Reports, 2015, 11, 3652-3658.	2.4	2
42	Removal of Mechanical-Polishing-Induced Surface Damages on 4H-SiC by Chemical Etching and its Effect on Subsequent Epitaxial Growth. Materials Science Forum, 2015, 821-823, 541-544.	0.3	3
43	Characterization of Damage Induced by Electric Discharge Machining and Wiresawing with Loose Abrasive at Subsurface of SiC Crystal. Materials Science Forum, 2014, 778-780, 362-365.	0.3	0
44	Comparison of slicing-induced damage in hexagonal SiC by wire sawing with loose abrasive, wire sawing with fixed abrasive, and electric discharge machining. Japanese Journal of Applied Physics, 2014, 53, 071301.	1.5	19
45	Removal of Mechanical-Polishing-Induced Surface Damages on 4H-SiC Wafers by Using Chemical Etching with Molten KCl+KOH. Materials Science Forum, 2014, 778-780, 746-749.	0.3	2
46	Cross-sectional observation of stacking faults in 4H-SiC by KOH etching on nonpolar \${ 1ar{1}00} \$ face, cathodoluminescence imaging, and transmission electron microscopy. Japanese Journal of Applied Physics, 2014, 53, 081301.	1.5	4
47	Correlation between etch pits formed by molten KOH+Na2O2 etching and dislocation types in heavily doped n+-4H–SiC studied by X-ray topography. Journal of Crystal Growth, 2013, 364, 7-10.	1.5	13
48	GW24-e2387â€Cyclin-A2 promotes cardiac self-repair via the recruitment of cardiac stem cells after myocardium infarction. Heart, 2013, 99, A10.1-A10.	2.9	0
49	GW24-e2389â€Delivery of AAV9 cyclin-A2 via hyaluronic acid hydrogel induces cardiac regeneration as well as improves cardiac function <i>in vivo</i> post mycardial infarction. Heart, 2013, 99, A25.3-A26.	2.9	Ο
50	Different Dissociation Behavior of [11-20] and Non-[11-20] Basal Plane Dislocations in 4H-SiÐi under Electron Beam Irradiation. Materials Science Forum, 2012, 725, 45-48.	0.3	0
51	Variation of Etch Pit Size by Screw Dislocation Tilt in 4H-SiC Wafer. Materials Science Forum, 2012, 717-720, 367-370.	0.3	4
52	Influence of substrate nitridation on GaN and InN growth by plasma-assisted molecular-beam epitaxy. Journal of the Ceramic Society of Japan, 2012, 120, 513-519.	1.1	3
53	Dislocation Revelation from (\$000ar{1}\$) Carbon-face of 4H-SiC by Using Vaporized KOH at High Temperature. Applied Physics Express, 2012, 5, 075601.	2.4	12
54	Transmission Electron Microscopy Analysis of a Threading Dislocation with \$c+a\$ Burgers Vector in 4H-SiC. Applied Physics Express, 2012, 5, 081301.	2.4	36

Υονςζήλο Υλό Υλό

#	Article	IF	CITATIONS
55	Molten KOH Etching with Na ₂ O ₂ Additive for Dislocation Revelation in 4H-SiC Epilayers and Substrates. Japanese Journal of Applied Physics, 2011, 50, 075502.	1.5	27
56	A simultaneous observation of dislocations in 4 <i>H</i> -SiC epilayer and n+-substrate by using electron beam induced current. Journal of Applied Physics, 2011, 109, .	2.5	6
57	Detection of Shallow Dislocations on 4H-SiC Substrate by Etching Method. Acta Physica Polonica A, 2011, 120, A-25-A-27.	0.5	2
58	Investigation on buffer layer for InN growth by molecular beam epitaxy. Journal of the Ceramic Society of Japan, 2010, 118, 152-156.	1.1	1
59	Nitrogen isotopic effect in Ga15N epifilms grown by plasma-assisted molecular-beam epitaxy. Scripta Materialia, 2010, 62, 516-519.	5.2	1
60	Surface effects on the luminescence degradation of hydride vapor-phase epitaxy-grown GaN induced by electron-beam irradiation. Journal of Vacuum Science and Technology A: Vacuum, Surfaces and Films, 2009, 27, 611-613.	2.1	8
61	Periodic supply of indium as surfactant for N-polar InN growth by plasma-assisted molecular-beam epitaxy. Applied Physics Letters, 2009, 95, .	3.3	6
62	Growth of colorless transparent GaN single crystals on prismatic GaN seeds using a Ga melt and Na vapor. Materials Research Bulletin, 2009, 44, 594-599.	5.2	22
63	Growth and characterization of isotopic ^{nat} Ga ¹⁵ N by molecularâ€beam epitaxy. Physica Status Solidi C: Current Topics in Solid State Physics, 2009, 6, S707.	0.8	1
64	Impact of electron beam irradiation on the cathodoluminescence intensity for ZnO and GaN. Journal of Materials Science: Materials in Electronics, 2008, 19, 307-310.	2.2	9
65	InN Growth by Plasma-Assisted Molecular Beam Epitaxy with Indium Monolayer Insertion. Crystal Growth and Design, 2008, 8, 1073-1077.	3.0	7
66	Photoluminescence and x-ray diffraction measurements of InN epifilms grown with varying Inâ^•N ratio by plasma-assisted molecular-beam epitaxy. Applied Physics Letters, 2008, 92, 211910.	3.3	5
67	Luminescence of GaN single crystals prepared by heating a Ga melt in Na–N2 atmosphere. Crystal Research and Technology, 2007, 42, 713-717.	1.3	1
68	The influence of indium monolayer insertion on the InN epifilm grown by plasma-assisted molecular beam epitaxy. Journal of Crystal Growth, 2007, 301-302, 521-524.	1.5	2
69	Effect of the oblique excitation and detection on the cathodoluminescence spectra. Materials Science in Semiconductor Processing, 2006, 9, 19-24.	4.0	0
70	Cathodoluminescence characterization of GaN quantum dots grown on 6H–SiC substrate by metal-organic chemical vapor deposition. Scripta Materialia, 2006, 55, 679-682.	5.2	4
71	Blue-Green Light Emission from a-SiC x :H-Based Fabry–Perot Microcavities. Chinese Physics Letters, 2006, 23, 482-485.	3.3	1
72	GaN nanodot fabrication by implant source growth. Microelectronics Journal, 2005, 36, 456-459.	2.0	3

#	Article	IF	CITATIONS
73	Dislocation Revelation in Highly Doped N-Type 4 <i>H</i> -SiC by Molten KOH Etching with Na ₂ O ₂ Additive. Materials Science Forum, 0, 679-680, 290-293.	0.3	9
74	Dislocation Analysis in Highly Doped n-Type 4 <i>H</i> -SiC by Using Electron Beam Induced Current and KOH+Na ₂ O ₂ Etching. Materials Science Forum, 0, 679-680, 294-297.	0.3	9
75	Dislocation Formation in Epitaxial Film by Propagation of Shallow Dislocations on 4H-SiC Substrate. Materials Science Forum, 0, 717-720, 383-386.	0.3	6
76	Characterization of Dislocation Structures in Hexagonal SiC by Transmission Electron Microscopy. Materials Science Forum, 0, 725, 11-14.	0.3	1
77	Electron Beam Induced Current Observation of Dislocations in 4H-SiC Introduced by Mechanical Polishing. Materials Science Forum, 0, 725, 23-26.	0.3	0
78	Large-Area Mapping of Dislocations in 4H-SiC from Carbon-Face (000-1) by Using Vaporized KOH Etching near 1000 °C. Materials Science Forum, 0, 740-742, 829-832.	0.3	2
79	Characterization of Threading Edge Dislocation in 4H-SiC by X-Ray Topography and Transmission Electron Microscopy. Materials Science Forum, 0, 778-780, 366-369.	0.3	1
80	Dislocation Revelation for 4H-SiC by Using Vaporized NaOH: A Possible Way to Distinguish Edge, Screw and Mixed Threading Dislocations by Etch Pit Method. Materials Science Forum, 0, 778-780, 346-349.	0.3	3
81	Elementary Screw and Mixed-Type Dislocations in 4H-SiC Characterized by X-Ray Topography Taken with Six Equivalent 11-28 <i>g</i> -Vectors and a Comparison to Etch Pit Evaluation. Materials Science Forum, 0, 897, 185-188.	0.3	3
82	Dislocation Revelation and Categorization for Thick Free-Standing GaN Substrates Grown by HVPE. Materials Science Forum, 0, 897, 707-710.	0.3	2
83	AFM Observation of Etch-Pit Shapes on β-Ga ₂ O ₃ (001) Surface Formed by Molten Alkali Etching. Materials Science Forum, 0, 1004, 512-518.	0.3	5